

Gastrodin exerts robust neuroprotection in the postischemic brain via its protective effect against Zn²⁺-toxicity and its anti-oxidative effects in astrocytes

Lidan Luo^{a,b,†}, Seung-Woo Kim^{b,c,†}, Hye-Kyung Lee^{a,b}, Il-Doo Kim^{a,b}, Hahnbie Lee^{a,b} and Ja-Kyeong Lee^{a,b}

^aDepartment of Anatomy, Inha University School of Medicine, Incheon, Republic of Korea; ^bMedical Research Center, Inha University School of Medicine Incheon, Incheon, Republic of Korea; ^cDepartment of Biomedical Sciences, Inha University School of Medicine, Incheon, Republic of Korea

ABSTRACT

Gastrodin (GAS) is a predominant bioactive constituent of the Chinese herbal medicine Tianma (*Gastrodia elata* Blume). Many authors have reported GAS has the beneficial effect on diverse diseases of the CNS, including epilepsy, Alzheimer's disease, Parkinson's disease, and cerebral ischemia. Here, we report GAS exhibited a robust neuroprotective effect in an Sprague-Dawley rat model of stroke (transient middle cerebral artery occlusion, tMCAO), and show that the underlying molecular mechanism involves its protective effect against Zn²⁺-toxicity and its anti-oxidative effects in astrocytes. Intraperitoneal administration of GAS (40 mg/kg) after MCAO reduced mean infarct volume to 30.1 ± 5.9% of that of MCAO controls and this neuroprotective effect was accompanied by neurological function recoveries which was measured using modified neurological severity score (mNSS). Interestingly, GAS induced up-regulation and nuclear translocation of Nrf2, and subsequently increased the expressions of anti-oxidative genes, such as, HO-1 and GCLM, in astrocytes. Furthermore, GAS co- or pre-treatment markedly suppressed Zn²⁺-induced cell death caused by excessive ROS production and PARP-1 induction. We found that GAS suppressed p67 expression and PAR formation in astrocytes, which might underlie the anti- Zn²⁺-toxicity and anti-oxidative effects of GAS in astrocytes. These findings indicate GAS protects astrocytes from Zn²⁺-induced toxicity and oxidative stress and these effects contribute to its neuroprotective effects in the postischemic brain.

ARTICLE HISTORY

Received 25 September 2018
Revised 5 November 2018
Accepted 12 November 2018

KEYWORDS



Gastrodin; MCAO; anti-Zn²⁺-toxicity; astrocyte; neuroprotection

Introduction

Gastrodin (GAS) is the main phenolic compound derived from the roots of *Gastrodia elata* Blume, which has been used in East Asia to treat epilepsy, paralysis, vertigo, headache, and convulsions (Park et al. 2011). It has been reported that GAS exerted neuroprotective effects in rat model of cerebral ischemic injury (Liu et al. 2016). GAS is able to cross the blood brain barrier (BBB) where it is metabolized to p-hydroxybenzyl alcohol (Lin et al. 2008). In a previous study, GAS inhibited oxygen-glucose deprivation (OGD)-induced calcium and nitric oxide increases in hippocampal neuron (Zeng et al. 2006) and enhanced cell survival under hypoxic conditions by inhibiting excitotoxicity (Xu et al. 2007). In addition, in LPS-stimulated microglial cells, GAS exerted anti-inflammatory effects by inhibiting the phosphorylations of IκB and mitogen-activated protein kinase (MAPK) (Dai et al. 2011). Interestingly, long-term GAS treatment was found to improve memory impairment induced by IDPN (3,3'-Iminodipropionitrile), by normalizing the

serotonergic system (Wang et al. 2015). Various molecular mechanisms have been proposed to explain the anti-oxidative effects of GAS, these include, attenuation of catalase reduction, increased superoxide dismutase (SOD) expression (Zhao et al. 2012) and the translocation of Nrf2 (nuclear factor erythroid-2-related factor) (Wang et al. 2014)

Zn²⁺ acts as a cofactor of various enzymes and transcription factors. In the central nervous system (CNS), Zn²⁺ accumulates in synaptic vesicles in neuron, and this accumulation maintains intracellular Zn²⁺ concentrations via ZnT3 (Cole et al. 1999). However, it has been reported that after transient forebrain ischemia, Zn²⁺ accumulation induces neuronal injury, and that this injury can be suppressed by chelating Zn²⁺ (Koh et al. 1996). Excessive Zn²⁺ release from neurons has a neurotoxic effects because it inhibits glyceraldehyde-3-phosphate dehydrogenase (GAPDH) and thus, reduced glycolysis and NAD production (Sheline et al. 2000). In addition, protein kinase C (PKC)-dependent intracellular

CONTACT Ja-Kyeong Lee  jklee@inha.ac.kr  Department of Anatomy, Inha University School of Medicine, Nam-gu, Inharo 100, Incheon, Republic of Korea
†They are equally contributed.

© 2018 The Author(s). Published by Informa UK Limited, trading as Taylor & Francis Group
This is an Open Access article distributed under the terms of the Creative Commons Attribution License (<http://creativecommons.org/licenses/by/4.0/>), which permits unrestricted use, distribution, and reproduction in any medium, provided the original work is properly cited.

ROS elevation has been reported in Zn^{2+} -treated cortical neurons (Noh et al. 1999). Zn^{2+} -mediated toxicity has also been reported in glial cells, for example, Zn^{2+} -mediated damage has been reported in astrocytes, and putatively attributed to ROS production and the inhibition of glutathione reductase (Bishop et al. 2007). In addition, Zn^{2+} released from neurons was observed to induce PARP-1 activation in astrocytes and to subsequently suppress glutamate uptake by astrocytes and aggravate neuronal injury (Suh et al. 2007).

Astrocytes have diverse functions, which include maintenance of fluid and ion balance, axon regeneration, neurotransmitter regulation, and energy substrate, neurotransmitter precursor, and growth factor release. In particular, in the postischemic brain, astrocytes regulate ischemic tolerance (Rossi et al. 2007). For example, astrocytes release glutamate and ATP, which contribute to neuroprotection by acting on sensors of ischemic tolerance in mildly ischemic brain (Li et al. 2008). Astrocytes also express NADPH oxidase, which activated by PKC and intracellular calcium and modulated by intracellular pH and play pivotal roles in pathophysiology of the CNS (Abramov et al. 2005). Interestingly, exacerbation of brain damage in GFAP null mice after permanent MCAO, further confirmed that astrocytes act in a neuroprotective manner in the postischemic brain (Nawashiro et al. 2000)

In the present study, we investigated whether GAS inhibits Zn^{2+} -induced oxidative stress in astrocytes in the postischemic brain using a rat model and sought to identify the molecular mechanisms responsible for its protective effects, particularly with respect to Nrf2 activation and the suppressions of NADPH oxidase, PARP-1 induction, and PAR formation in C6 astroglial cells.

Materials and methods

Experimental animals

Male Sprague–Dawley (SD) (8–9 weeks) rats were housed under controlled diurnal lighting conditions with free access to food and tap water. All animal studies were carried out in strict accordance with the Guide for the Care and Use of Laboratory Animals published by the National Institute of Health (NIH, USA 2011) and with ARRIVE guidelines (<http://www.nc3rs.org/ARRIVE>). The protocol of the animal experiment was reviewed and approved by the INHA University-Institutional Animal Care and Use Committee (INHA-IACUC) with respect to ethicality (Approval Number INHA-141124-337). MCAO was carried out as previously described (Kim et al. 2011).

Drug injection

GAS was purchased from Sigma-Aldrich (Sigma, St. Louis, MO), dissolved in dimethyl sulfoxide (DMSO) and administered intraperitoneally at 1 or 6 h post-MCAO. Rats were randomly allocated to five groups: a MCAO group, treatment-naive MCAO controls ($n=13$); a MCAO + GAS group, GAS-treated MCAO group ($n=53$), a GAS group, GAS-treated controls ($n=4$), a sham group, animals underwent surgery but not MCAO ($n=4$); and a normal group, treatment-naive control group ($n=4$). No animals died during surgery, but the mortality rate after surgery was 4.9% (4/82).

Infarct volume assessment

To measure infarct volumes, rats were sacrificed at 24 h post-MCAO and 2 mm brain coronal sections were obtained using a metallic brain matrix (RBM-40000, ASI, Springville, UT). Brain sections were immediately immersed in 2% 2,3,5-triphenyltetrazolium chloride (TTC; Sigma, St. Louis, MO) for 15 min at 37°C and stored in 4% paraformaldehyde (PFA; Sigma, St. Louis, MO). Infarct volumes were measured using the Scion Image Program (Frederick, MD). To account for edema and shrinkage, volumes of ischemic lesions were calculated as (contralateral hemisphere volume – (ipsilateral hemisphere volume – measured injury volume)). Infarct volumes were quantified (in mm^3) by multiplying summed infarct areas of consecutive sections by section thickness.

Behavioral testing

Neurological deterioration was evaluated using modified Neurological Severity Scores (mNSSs) at 24 h post-MCAO, as previously described (Kim et al. 2011). mNSS were calculated by summing the motor, sensory, reflex and balance test scores, and ranges from 0 to 18 (0 = normal, 18 = maximum deficit).

C6 astroglial cell culture and Zn^{2+} treatment

C6 astroglial cells were grown in Dulbecco's modified Eagle's medium (DMEM; Sigma, St. Louis, MO) supplemented with 5% fetal bovine serum (FBS; Thermo, Waltham, MA) at 37°C in a humidified 5% CO_2 /95% air and atmosphere. C6 cells (5×10^4 /well) were treated with 10, 25, 50 or 100 μM of zinc sulfate (Sigma, St. Louis, MO) for 6, 12, or 24 h in serum-free DMEM or with 25, 50, 100, or 200 μM of Zn^{2+} for 15 min in HCSS (HEPES controlled salt solution).

Reactive oxygen species quantifications

C6 cells (5×10^4) were seeded into 24-well plates, cultured for 24 h, treated with Zn^{2+} and/or GAS for the indicated times, and incubated in DMEM containing $5 \mu M$ of 5-(and-6)-chloromethyl-2',7'-dichlorodihydrofluorescein diacetate (CM-H2DCFDA; Thermo Fisher Scientific, Waltham, MA) for 30 min. After washing in PBS, fluorescence and differential interference contrast images were obtained using a Zeiss microscope (Oberkochen, Germany). Fluorescence intensity was quantified using ImageJ software (<http://rsbweb.nih.gov/ij/>).

Cell viability assays

After Zn^{2+} -treatments, cell viabilities were determined using a MTT (3-[4,5-dimethylthiazol-3-yl] 2,5-diphenyltetrazolium bromide; Sigma, St. Louis, MO) assay. After Zn^{2+} -treatment for 24 h, C6 cells were incubated with $500 \mu g/ml$ of MTT for 60 min. Formazan crystals were solubilized using $300 \mu l$ of DMSO (Sigma, St. Louis, MO) and optical densities were read at 550 nm.

Immunoblot analysis

C6 cells were washed with cold PBS and lysed with RIPA buffer (50 mM Tris-HCl (pH 7.4), 0.5% NP40, 0.5% Triton X-100, 0.25% sodium deoxycholate, 150 mM NaCl, and 1 complete Mini protease inhibitor cocktail tablet (Roche Diagnostics, Basel, Switzerland)). Cell lysates were centrifuged at $17,500 g$ for 10 min at $4^\circ C$. Total protein contents were measured using BCA protein assay kits (Thermo Fisher Scientific, Waltham, MA). The primary antibodies used were as follows: anti-PARP-1 (1: 3000; Santa Cruz Biotechnology, Santa Cruz, CA), anti-p67 (1:3000; Santa Cruz Biotechnology, Santa Cruz, CA), anti-PAR (1:3000; Trevigen, Gaithersburg, MD) and anti- α -Tubulin (1:5000; Cell Signaling, Danvers, MA). Primary antibodies were detected using a chemiluminescence kit (Merck Millipore, Darmstadt, Germany) using horseradish peroxidase-conjugated secondary antibody (1:4000; Merck Millipore, Darmstadt, Germany).

Measurement of NAD levels

C6 cells were treated with 0.125 ml of $0.5 N HClO_4$ (Sigma, St. Louis, MO), which was then neutralized with KOH (125 mM). Supernatants obtained by centrifuging for 5 min at $10,000 g$ were reacted with a premix containing $0.9 mM$ phenazine ethosulfate (Sigma, St. Louis, MO), $0.1 mM$ MTT, 5.8% ethanol, $0.5 mM$ EDTA, and 4 U of alcohol dehydrogenase (Sigma-Aldrich, St. Louis, MO) in $61 mM$ Gly-Gly buffer (pH 7.4), in the dark at $37^\circ C$

for 30 min. Absorbance was measured at 550 nm and result was normalized with respect to protein concentrations determined using a BCA assay kit (Thermo Scientific, Waltham, MA).

Statistical analysis

Statistical analysis was performed using by analysis of variance (ANOVA) followed by the Newman-Keuls test. Results are presented as means \pm SEMs, and statistical significance was accepted at the 5% level.

Results

Neuroprotective effects of GAS in the postischemic brain

GAS (20, 40, or 80 mg/kg) was administered intraperitoneally at 1 or 6 h post-MCAO to rats and infarct volumes were assessed at 1 d post-MCAO. GAS (40 or 80 mg/kg) administered at 1 h post-MCAO reduced infarct volumes to $22.2 \pm 5.6\%$ ($n = 5$, $p < 0.01$), and $56.8 \pm 12.6\%$ ($n = 5$, $p < 0.01$), respectively, of that of treatment naïve MCAO controls (Figure 1(a and b)). When 40 mg/kg of GAS was administered at 6 h post-MCAO, mean infarct volume reduced to $43.9 \pm 9.6\%$ ($n = 4$, $p < 0.05$) of that of treatment naïve MCAO controls (Figure 1(a and b)). These results show GAS exerted a neuroprotective effect against ischemic injury with a wide therapeutic window.

Improvements in neurological deficits after MCAO by GAS

mNSSs were measured at 1 d post MCAO. The mean mNSS score of treatment-naïve MCAO controls was 13.7 ± 0.4 ($n = 8$) (Figure 2). The administration of GAS at 20, 40, or 80 mg/kg at 1 h post-MCAO reduced mNSSs to 8.3 ± 0.5 ($n = 7$), 4.3 ± 0.9 ($n = 4$), and 8.3 ± 0.9 ($n = 4$), respectively (Figure 2), and GAS at these same levels administered at 6 h post-MCAO reduced mNSS scores to 9.0 ± 2.3 ($n = 4$), 6.0 ± 0.7 ($n = 4$), and 8.5 ± 2.1 ($n = 4$), respectively (Figure 2). Accordingly, GAS administration was found to be accompanied by marked reductions in neurological deficits. In addition, we found pH, PaO_2 , $PaCO_2$, and glucose levels were similar in GAS-treated and -untreated animals (Table 1).

Suppression of Zn^{2+} -induced C6 astroglial death by GAS

To determine whether GAS has protective effects protects against Zn^{2+} -toxicity, we examined the viabilities

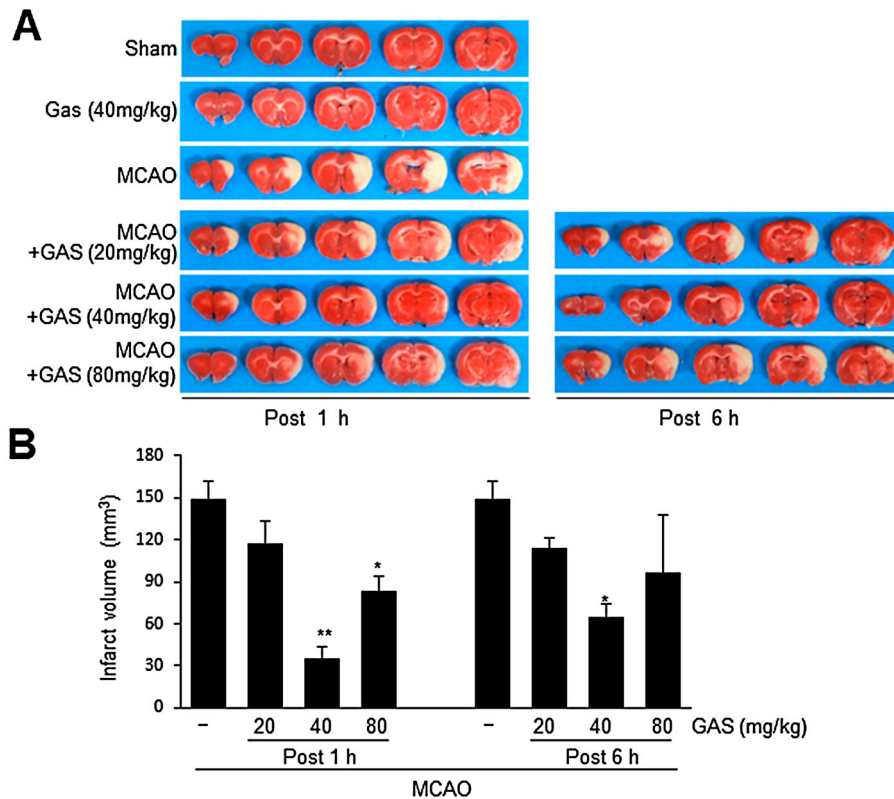


Figure 1. Suppression of infarct formation by GAS in the posts ischemic brain. GAS (20, 40, or 80 mg/kg) was administered intraperitoneally at 1 h or 6 h post-MCAO (60 min), and infarct volumes were measured by TTC staining. (B) Mean infarction volumes were measured at 1 d post-MCAO. Representative images of infarction in coronal brain sections are presented (A) and quantitative data are presented as means \pm SEMs (B). Sham, sham-operated control rats ($n = 4$); GAS, GAS-administered control rats ($n = 4$); MCAO, treatment-naïve MCAO control rats ($n = 8$); MCAO + GAS, GAS-administered MCAO rats ($n = 29$). * $p < 0.05$, ** $p < 0.01$ versus treatment-naïve MCAO controls.

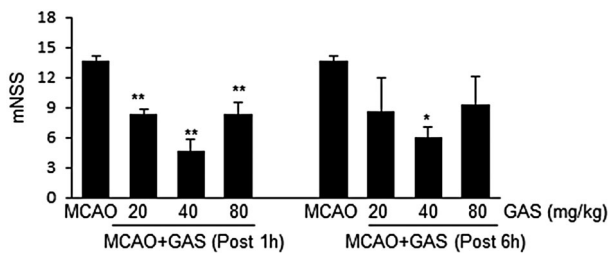


Figure 2. Improvement of neurological deficits by GAS. GAS (20, 40, or 80 mg/kg) was administered intraperitoneally at 1 h or 6 h post-MCAO and neurological deficits were evaluated using mNSS at 1 d post MCAO. MCAO, treatment-naïve MCAO control rats ($n = 8$); MCAO + GAS, GAS-administered MCAO rats ($n = 27$). * $p < 0.05$, ** $p < 0.01$ versus treatment-naïve MCAO controls.

of C6 cells, an astrocyte cell line, after treating them with Zn²⁺ for 15 min to 24 h in the presence or absence of GAS. When C6 cells were treated with Zn²⁺ (50 μ M) for 24 h, mean cell viability was $50.9 \pm 2.8\%$ ($n = 4$) (Figure 3(a)). However, co-treatment with GAS (50, 100, or 250 μ M) significantly increased cell viability, and at a GAS concentration of 100 μ M, mean cell viability after

Table 1. Physiological parameters.

	Control group		Ischemia group	
	Base	GAS	MCAO	MCAO + GAS
Temperature, °C	37.08 \pm 0.17	37.0 \pm 0.13	37.04 \pm 0.14	37.04 \pm 0.12
pH	7.64 \pm 0.04	7.42 \pm 0.00	7.58 \pm 0.03	7.40 \pm 0.02
pO ₂ , mmHg	145.8 \pm 19.2	163.2 \pm 12.6	150.22 \pm 6.66	166.6 \pm 9.77
pCO ₂ , mmHg	32.16 \pm 1.95	32.3 \pm 0.96	39.06 \pm 1.23	30.04 \pm 0.70
Glucose, mg/dL	109.80 \pm 5.63	103.4 \pm 2.92	109.6 \pm 5.19	95.6 \pm 6.90

Values are mean SD ($n = 4$). One-way analysis of variance revealed no significant intergroup difference for any variable.

24 h was $74.9 \pm 3.7\%$ ($n = 4$) (Figure 3(a)). In addition, pre-treating C6 cells with GAS (50, 100, or 250 μ M) for 6 h before Zn²⁺ treatment increased cell viability slightly (Figure 3(b)). Similarly, C6 cell viability after acute Zn²⁺ treatment (200 μ M, 15 min) was also enhanced to $67.7 \pm 5.6\%$ ($n = 4$) by pre-treating cells with GAS (100 μ M, 6 h) or to $77.8 \pm 7.0\%$ ($n = 4$) by post-treating cells with GAS (250 μ M, 24 h), respectively, as compared with that of treatment-naïve Zn²⁺ control cells, $50.8 \pm 2.0\%$ ($n = 4$) or $53.3 \pm 3.3\%$ ($n = 4$) (Figure 3(c and d)). These results shows GAS had a prominent protective effect against acute or chronic Zn²⁺-induced C6 cell death.

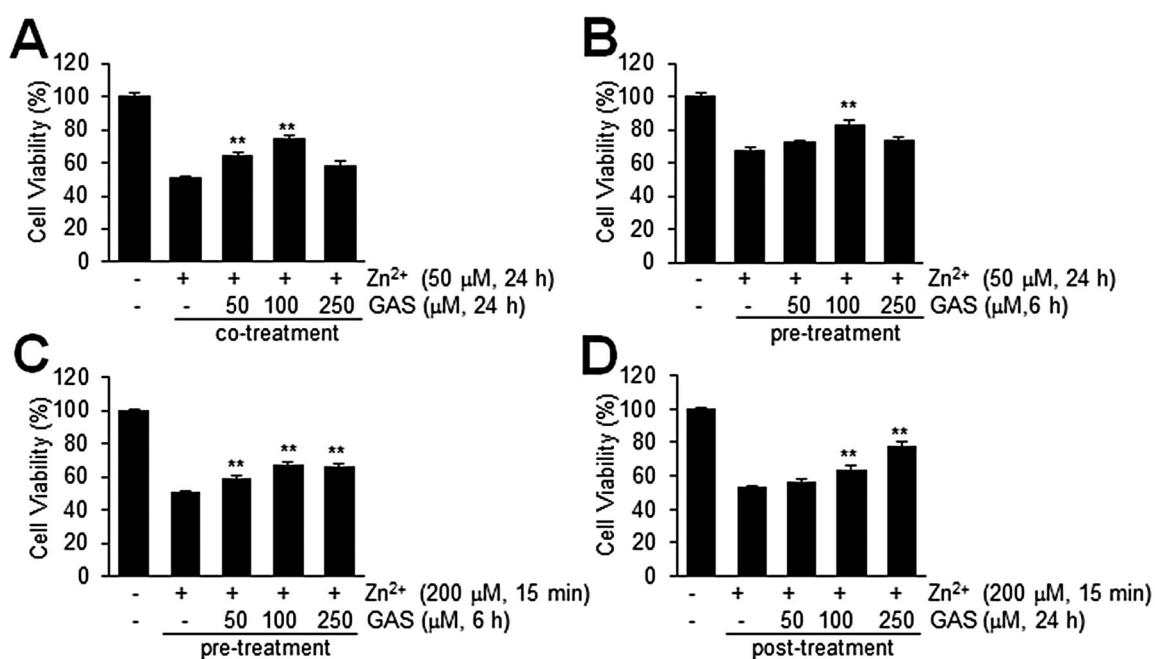


Figure 3. Increased cell viability by GAS in Zn²⁺-treated C6 cells. (A, B) C6 cells were co-treated with 50 μM of Zn²⁺ and GAS (50, 100, or 250 μM) for 24 h (A) or treated with 50 μM of Zn²⁺ for 24 h with or without pre-treatment of GAS (50, 100, or 250 μM) for 6 h (B). (C, D) C6 cells were treated with 200 μM of Zn²⁺ for 15 min with or without 6 h of GAS pretreatment (50, 100, or 250 μM) (C) or post-treated with GAS at these concentrations for 24 h (D). Cell viabilities were measured using a MTT assay. Results are presented as means ± SEMs ($n = 4$) ** $p < 0.01$ versus Zn²⁺-treated controls.

Up-regulation and nuclear translocation of Nrf2 by GAS in C6 astroglial cells

Since it has been reported that many phytochemicals regulate Nrf2 (Surh et al. 2005), we investigated whether GAS induces the expression and/or the nuclear translocation of Nrf2 in C6 cells. Total intracellular levels of Nrf2 started to increase after 3 h of GAS (100 μM) treatment and then progressively increased over the following 3, 6, 9, or 12 h (Figure 4(a)). Furthermore, the nuclear translocation of Nrf2 was detected after 3 h of GAS treatment, and its nuclear levels further increased of the next 9 h (Figure 4(b)). Double fluorescence immunostaining with anti-Nrf2 and DAPI showed that GAS induced the nuclear translocation of Nrf2 at 3 h and further increased the nuclear translocation for 9 h, when Nrf2 was also detected in cytoplasm (Figure 4(d)). Expressions of anti-oxidative genes, e.g. HO-1 and GCLM, were also induced by GAS (100 μM) (Figure 4(e)). These results indicated that GAS induced the up-regulation and nuclear translocation of Nrf2 and increased the expression of downstream anti-oxidative genes.

GAS inhibited ROS generation and NAD depletion in Zn²⁺-treated C6 cells

Since, it has been reported excessive Zn²⁺ triggers ROS production (Noh and Koh 2000), we examined

Zn²⁺-induced ROS production in C6 cells in the presence or absence of GAS. Intracellular ROS levels were visualized using CM-H2DCFDA and found to be significantly increased after 12 h of Zn²⁺ (50 μM) treatment (Figure 5(a)). However, pre-treatment with 50 or 100 μM of GAS for 12 h reduced Zn²⁺-induced ROS production to $68.8 \pm 4.7\%$ and $41.6 \pm 3.7\%$, respectively (Figure 5(b)). Similarly, it was reduced to $83.14 \pm 5.7\%$ and $72.8 \pm 9.0\%$, respectively, measured at 24 h after Zn²⁺ (50 μM) treatment (Figure 5(b)). Zn²⁺ (50 μM) was also observed to increase p67 (an NADPH oxidase subunit) levels in C6 cells (Noh and Koh 2000) and these were also suppressed by GAS (100 μM) pre-treatment (Figure 5(c)). In addition, it has been reported Zn²⁺ also induces PARP-1 activation, which depletes NAD⁺ and ATP and causes cell death (Sheline et al. 2003). PARP-1 up-regulation was observed in Zn²⁺-treated C6 cells and found to be significantly suppressed by pre-treating cells with GAS (50 or 100 μM) for 6 h (Figure 5(d and e)). Furthermore, subsequent PAR formation and NAD depletion by Zn²⁺ were suppressed by pre-treating cells with GAS at 50 or 100 μM for 6 h. These results indicate GAS suppressed Zn²⁺-induced ROS production and PAR formation by inhibiting p67 and PARP-1 induction in Zn²⁺-treated C6 cells.

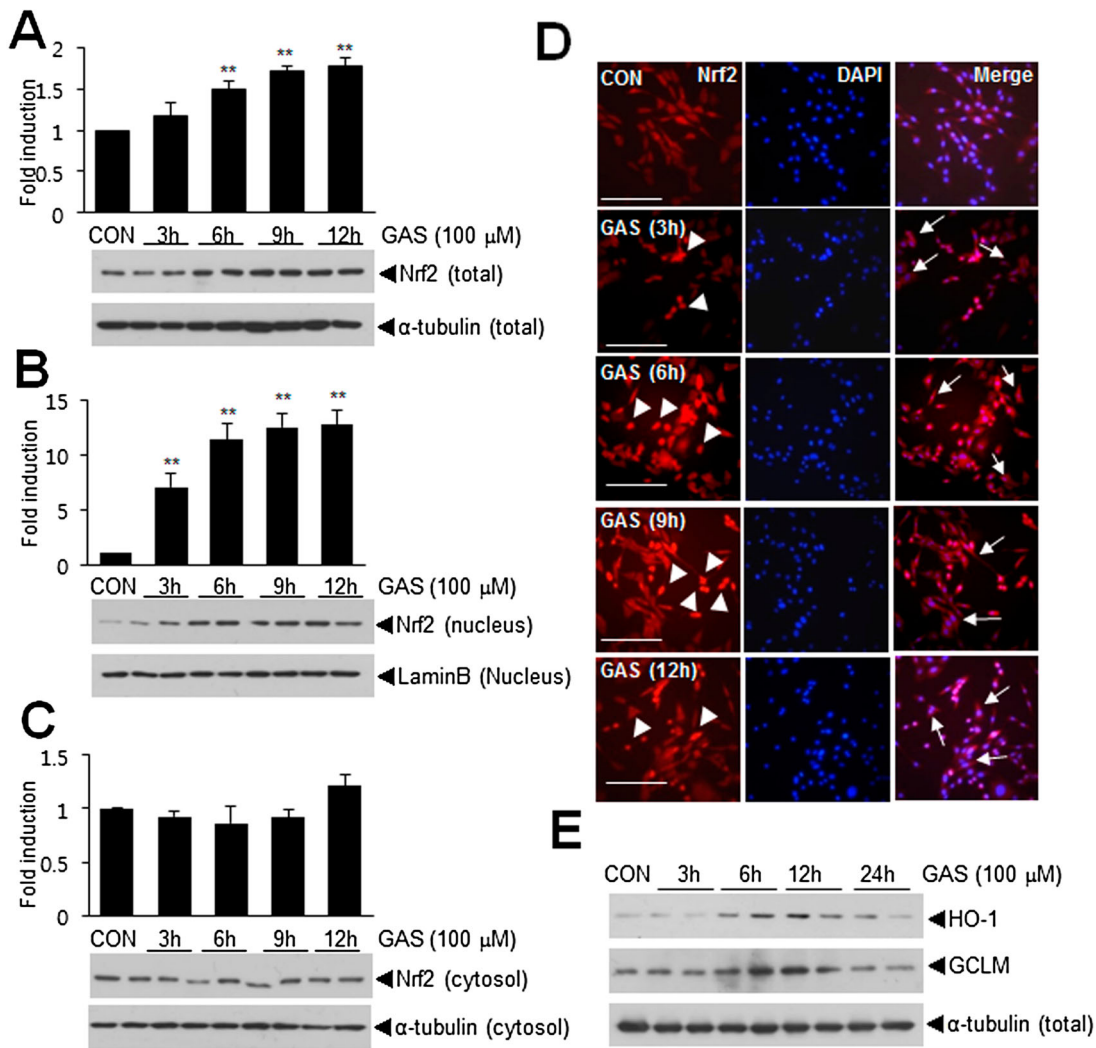


Figure 4. The up-regulation and nuclear translocation of Nrf2 by GAS. (A, B) C6 cells were treated with 100 μ M of GAS for 3, 6, 9, or 12 h and total (A), nuclear (B) and cytoplasmic Nrf2 levels (C) were determined by immunoblotting. (D) Double fluorescent staining was performed using anti-Nrf2 antibody and DAPI after treating C6 cells with GAS (100 μ M) for 3, 6, 9, or 12 h. Arrowheads indicate Nrf2 translocation from cytoplasm to nucleus and arrows indicate cytoplasmic localization of Nrf2. (E) C6 cells were treated with 100 μ M GAS for 3, 6, 9, or 12 h and protein levels of HO-1, GCLM, and α -tubulin were determined by immunoblotting. The scale bar represents 100 μ m. Results are presented as means \pm SEMs ($n = 4$) ** $p < 0.01$ versus treatment naive controls.

Discussion

GAS is a phenolic glycoside and a main bioactive constituent of *Rhizoma Gastrodiae*, which has been traditionally used to treat various diseases. Furthermore, numerous scientific studies have reported GAS has neuroprotective effects in CNS disorders, such as, Alzheimer's disease (Hu et al. 2014), Parkinson's disease (Wang et al. 2014), and cerebral ischemia (Zeng et al. 2006). In particular, GAS has been reported to have neuroprotective effects in an animal model of transient MCAO, wherein GAS (15, 30, and 60 mg/kg) was pre-treated for 7 d (Liu et al. 2016). However, in the present study, we observed a greater neuroprotective effect after a single bolus (40 mg/kg, i.p.) administration of GAS at 1 or 6 h after MCAO (Figure 1(b)). In addition,

we found GAS protected astrocytes from Zn^{2+} toxicity and had anti-oxidative effects. Although GAS has been previously reported to exhibit prominent neuroprotective effects in a MCAO model (Liu et al. 2016), we are the first to report that it protects astrocytes against toxic effects of Zn^{2+} , which might contribute to its robust protective effects in MCAO animal model.

During the early stage after stroke, massive neuronal cell damage is caused by excitotoxicity and Zn^{2+} overload, (Lipton 1999) and subsequent inflammation and apoptosis over a few hours to days aggravate ischemic brain damage (Graham and Chen 2001). In neurons, excessive Zn^{2+} accumulation and its oxidative and excitotoxic effects cause severe damage by inhibiting GAPDH, which reduces glycolysis and NAD levels

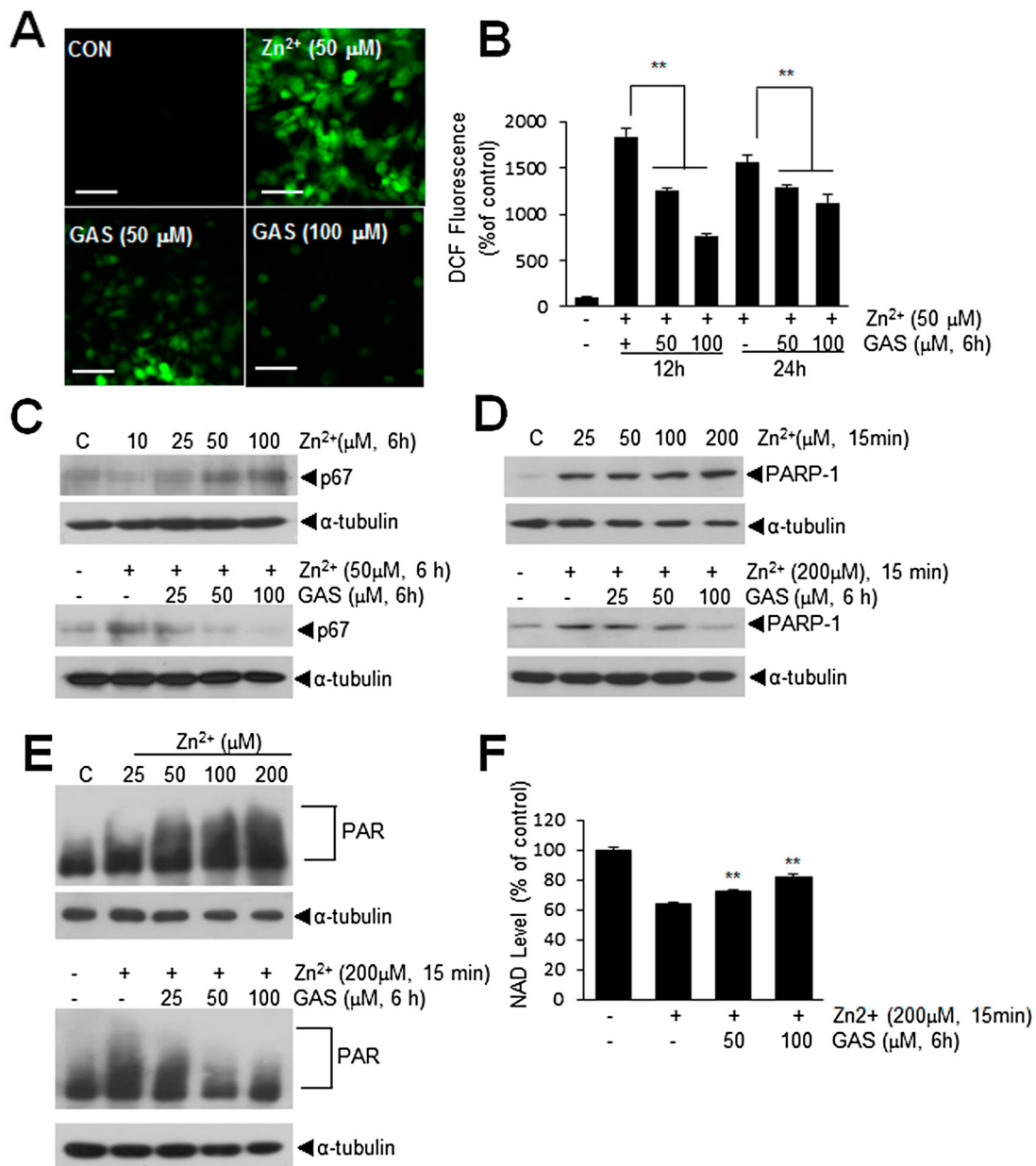


Figure 5. Suppressions of Zn²⁺-mediated inductions of ROS, p67, and PARP-1 in C6 astroglial cells. (A, B) C6 cells were treated with Zn²⁺ (50 μM) for 12 or 24 h with or without pre-treating GAS (50 or 100 μM) for 6 h, and intracellular ROS productions were measured using CM-H₂DCFDA. (C) Protein levels of p67 were measured after 6 h of Zn²⁺ treatment (10, 25, 50, 100 μM) and after 50 μM of Zn²⁺ treatment with pre-treating cells with GAS (25, 50, 100 μM) for 6 h. (D-E) PARP-1 and PAR levels were measured at 60 min after Zn²⁺ (25, 50, 100, 200 μM) treatment and at 60 min after 200 μM of Zn²⁺ treatment with pre-treating GAS (25, 50, 100 μM) for 6 h prior to Zn²⁺ treatment. (F) NAD levels were measured in C6 cells at 6 h after Zn²⁺-treatment (200 μM, 15 min) with or without GAS pre-treatment (50 or 100 μM, 6 h). Quantitative data are presented as means ± SEMs. ***p* < 0.01 versus Zn²⁺-treated controls. The scale bar represents 50 μm.

(Sheline et al. 2000). Although astrocytes are more resistant than neurons to high levels of Zn²⁺ (Dineley et al. 2000), ROS production and glutathione formation are nevertheless impaired (Noh and Koh 2000; Bishop et al. 2007). In the present study, we found GAS markedly suppressed Zn²⁺-induced ROS production and Zn²⁺-induced elevation of the levels of the p67 subunit of NADPH oxidase in astrocytes, indicating the anti-oxidative

effects of GAS underlie, at least in part, its amelioration of the toxic effects of Zn²⁺ in astrocytes.

The anti-oxidative effects of GAS have been reported in several cell types including neurons, in which Nrf2 (Wang et al. 2014), HO-1, p38 MAPK (Jiang et al. 2014), and ERK (Zhao et al. 2012) were shown to be involved. In the present study, GAS increased Nrf2 expression and its nuclear translocation in C6 astrocytes and maintained this

over 12 h of treatment (Figure 4(a and b)) and also induced the expressions of antioxidant genes, such as, HO-1 and GCLM (Figure 4(c)). However, we found astrocytes need to be treated with GAS at a higher dose (100 μ M) compared to other cell types in previous studies (25–30 μ M) (Zhao et al. 2012) and it might be due to cell type differences. In addition, rapid nuclear translocation of Nrf2 induced by GAS prompted us to speculate GAS-mediated Nrf2 translocation might be able to inhibit inflammatory response by promoting p300 to Nrf2 binding rather than p300 to p65 binding, as we previously reported for ethyl pyruvate and curcumin (Kim et al. 2013; Lee et al. 2016). Further study is needed to confirm that the anti-inflammatory effects exert by this mechanism also contribute to the neuroprotective effect of GAS.

We also observed GAS significantly suppressed Zn²⁺-mediated PARP-1 induction and subsequent PAR formation in astrocytes (Figure 5(e)). Although, astrocytes are more resistant to ischemia than neurons, excess Zn²⁺ release from a subset of neurons after stroke promotes astrocyte hypoxic cell death by modifying PARP-1 and upregulating HIF-1 α (Pan et al. 2013). Furthermore, PARP-1 activation inhibits glutamate uptake by astrocytes and leads to NAD⁺ and ATP depletion (Suh et al. 2007). We also showed increase in NAD levels in astrocytes by GAS. Therefore, astrocyte damage induced by excessive Zn²⁺ release from neuron further exacerbates neuronal damage through this vicious cycle in the post-ischemic brain. Since astrocytes are known to have beneficial effects in the postischemic brain, such as, anti-excitotoxic effects, and releasing neurotrophins during the acute phase, and contribute to angiogenesis, neurogenesis, and synaptogenesis during the recovery phase (Liu et al. 2016), GAS-mediated protective effects on astrocytes contribute to its robust neuroprotective effects observed in MCAO model.

Taken together, our results show GAS suppressed Zn²⁺-induced astrocytic cell death by inhibiting the inductions of p67 and PARP-1, and that *in vivo* suppressed infarct formation, and improved neurological deficits. Because Zn²⁺ toxicity is a known component of various neurological diseases, such as, trauma and epilepsy, we suggest further studies be undertaken to investigate the merits of GAS in targeting Zn-induced toxicity.

Disclosure statement

No potential conflict of interest was reported by the authors.

Funding

This work was financed by an Inha University Research Grant (2016) (54677-01) (to J-KL). The funders are not involved in

the design of the study, collections and analysis of data, and in writing the manuscript.

References

- Abramov AY, Jacobson J, Wientjes F, Hothersall J, Canevari L, Duchen MR. 2005. Expression and modulation of an NADPH oxidase in mammalian astrocytes. *J Neurosci*. 25:9176–9184.
- Bishop GM, Dringen R, Robinson SR. 2007. Zinc stimulates the production of toxic reactive oxygen species (ROS) and inhibits glutathione reductase in astrocytes. *Free Radic Biol Med*. 15:1222–1230.
- Cole TB, Wenzel HJ, Kafer KE, Schwartzkroin PA, Palmiter RD. 1999. Elimination of zinc from synaptic vesicles in the intact mouse brain by disruption of the ZnT3 gene. *Proc Natl Acad Sci USA*. 96:1716–1721.
- Dai JN, Zong Y, Zhong LM, Li YM, Zhang W, Bian LG, Ai QL, Liu YD, Sun J, Lu D, et al. 2011. Gastrodin inhibits expression of inducible NO synthase, cyclooxygenase-2 and proinflammatory cytokines in cultured LPS-stimulated microglia via MAPK pathways. *PLoS One*. 6:e21891.
- Dineley KE, Scanlon JM, Kress GJ, Stout AK, Reynolds JJ. 2000. Astrocytes are more resistant than neurons to the cytotoxic effects of increased [Zn(2+)](i). *Neurobiol Dis*. 7:310–320.
- Graham SH, Chen J. 2001. Programmed cell death in cerebral ischemia. *J Cereb Blood Flow Metab*. 21:99–109.
- Hu Y, Li C, Shen W. 2014. Gastrodin alleviates memory deficits and reduces neuropathology in a mouse model of Alzheimer's disease. *Neuropathology*. 34:370–377.
- Jiang G, Hu Y, Liu L, Cai J, Peng C, Li Q. 2014. Gastrodin protects against MPP(+)-induced oxidative stress by up regulates heme oxygenase-1 expression through p38 MAPK/Nrf2 pathway in human dopaminergic cells. *Neurochem Int*. 75:79–88.
- Kim SW, Kim HJ, Shin JH, Kim ID, Lee JE, Han PL, Yoon SH, Lee JK. 2011. Robust protective effects of a novel multimodal neuroprotectant oxopropanoyloxy benzoic acid (a salicylic acid/pyruvate ester) in the postischemic brain. *Mol Pharmacol*. 79:220–228.
- Kim SW, Lee HK, Shin JH, Lee JK. 2013. Up-down regulation of HO-1 and iNOS gene expressions by ethyl pyruvate via recruiting p300 to Nrf2 and depriving It from p65. *Free Radic Biol Med*. 65:468–476.
- Koh JY, Suh SW, Gwag BJ, He YY, Hsu CY, Choi DW. 1996. The role of zinc in selective neuronal death after transient global cerebral ischemia. *Science*. 272:1013–1016.
- Lee H, Kim SW, Lee HK, Luo L, Kim ID, Lee JK. 2016. Upregulation of Nrf2–p300 mediates antiinflammatory effects of curcumin in microglia by downregulating p65–p300. *Animal Cells Syst (Seoul)*. 20:246–252.
- Li J, Liu W, Ding S, Xu W, Guan Y, Zhang JH, Sun X. 2008. Hyperbaric oxygen preconditioning induces tolerance against brain ischemia-reperfusion injury by upregulation of antioxidant enzymes in rats. *Brain Res*. 1210:223–229.
- Lin LC, Chen YF, Lee WC, Wu YT, Tsai TH. 2008. Pharmacokinetics of gastrodin and its metabolite p-hydroxybenzyl alcohol in rat blood, brain and bile by microdialysis coupled to LC-MS/MS. *J Pharm Biomed Anal*. 48:909–917.
- Lipton P. 1999. Ischemic cell death in brain neurons. *Physiol Rev*. 79:1431–1568.
- Liu B, Li F, Shi J, Yang D, Deng Y, Gong Q. 2016. Gastrodin ameliorates subacute phase cerebral ischemia-reperfusion injury

- by inhibiting inflammation and apoptosis in rats. *Mol Med Rep.* 14:4144–4152.
- Nawashiro H, Brenner M, Fukui S, Shima K, Hallenbeck JM. 2000. High susceptibility to cerebral ischemia in GFAP-null mice. *J Cereb Blood Flow Metab.* 20:1040–1044.
- Noh KM, Kim YH, Koh JY. 1999. Mediation by membrane protein kinase C of zinc-induced oxidative neuronal injury in mouse cortical cultures. *J Neurochem.* 72:1609–1616.
- Noh KM, Koh JY. 2000. Induction and activation by zinc of NADPH oxidase in cultured cortical neurons and astrocytes. *J Neurosci.* 20:RC111.
- Pan R, Chen C, Liu WL, Liu KJ. 2013. Zinc promotes the death of hypoxic astrocytes by upregulating hypoxia-induced hypoxia-inducible factor-1 α expression via poly(ADP-ribose) polymerase-1. *CNS Neurosci Ther.* 19:511–520.
- Park S, Kim DS, Kang S. 2011. *Gastrodia elata* blume water extracts improve insulin resistance by decreasing body fat in diet-induced obese rats: vanillin and 4-hydroxybenzaldehyde are the bioactive candidates. *Eur J Nutr.* 50:107–118.
- Rossi DJ, Brady JD, Mohr C. 2007. Astrocyte metabolism and signaling during brain ischemia. *Nat Neurosci.* 10:1377–1386.
- Sheline CT, Behrens MM, Choi DW. 2000. Zinc-induced cortical neuronal death: contribution of energy failure attributable to loss of NAD(+) and inhibition of glycolysis. *J Neurosci.* 20:3139–3146.
- Sheline CT, Wang H, Cai AL, Dawson VL, Choi DW. 2003. Involvement of poly ADP ribosyl polymerase-1 in acute but not chronic zinc toxicity. *Eur J Neurosci.* 18:1402–1409.
- Suh SW, Aoyama K, Alano CC, Anderson CM, Hamby AM, Swanson RA. 2007. Zinc inhibits astrocyte glutamate uptake by activation of poly(ADP-ribose) polymerase-1. *Mol Med.* 13:344–349.
- Surh YJ, Kundu JK, Na HK, Lee JS. 2005. Redox-sensitive transcription factors as prime targets for chemoprevention with anti-inflammatory and antioxidative phytochemicals. *J Nutr.* 135:2993S–3001S.
- Wang X, Tan Y, Zhang F. 2015. Ameliorative effect of gastrodin on 3,3'-iminodipropionitrile-induced memory impairment in rats. *Neurosci Lett.* 594:40–45.
- Wang XL, Xing GH, Hong B, Li XM, Zou Y, Zhang XJ, Dong MX. 2014. Gastrodin prevents motor deficits and oxidative stress in the MPTP mouse model of Parkinson's disease: involvement of ERK1/2-Nrf2 signaling pathway. *Life Sci.* 114:77–85.
- Xu X, Lu Y, Bie X. 2007. Protective effects of gastrodin on hypoxia-induced toxicity in primary cultures of rat cortical neurons. *Planta Med.* 73:650–654.
- Zeng X, Zhang S, Zhang L, Zhang K, Zheng X. 2006. A study of the neuroprotective effect of the phenolic glucoside gastrodin during cerebral ischemia in vivo and in vitro. *Planta Med.* 72:1359–1365.
- Zhao X, Zou Y, Xu H, Fan L, Guo H, Li X, Li G, Zhang X, Dong M. 2012. Gastrodin protect primary cultured rat hippocampal neurons against amyloid-beta peptide-induced neurotoxicity via ERK1/2-Nrf2 pathway. *Brain Res.* 1482:13–21.